J Mater Sci (2007) 42:5159–5164
DOI 10.1007/s10853-006-1288-9

Proximity-effect correction in electron-beam lithography on metal multi-layers

Hyunjung Yi · Joonyeon Chang

Received: 18 May 2005 / Accepted: 17 November 2006 / Published online: 26 April 2007
© Springer Science+Business Media, LLC 2007

Abstract We report a proximity-effect correction in electron beam patterning when fabricating a spin valve device with a junction size of 100 nm × 100 nm. Since the spin valve device has a stack of magnetic/non-magnetic/magnetic metal multi-layers on oxidized Si substrate, its proximity effect should be appropriately corrected to realize a nano-scale junction. ZEP 520A was chosen as an electron beam resist because its dry-etching resistance is high enough to serve as an etching mask in the post-process. A set of proximity parameters, α, β, and η of ZEP 520A coated metal multi-layers was evaluated by using the doughnut pattern method. A simulation was carried out based on given proximity parameters in order to obtain effective dose factors of each segment of the exposure pattern. The junction with a desired shape and size on a metal multi-layer was successfully fabricated with a help of efficient proximity-effect correction.

Introduction

The simple spin valve (SV) structure comprises a FM/NM/FM trilayer, where both FMs are ferromagnetic metal layers and NM is a Cu spacer [1, 2]. The fabrication of nano-sized magnetic multi-layer junctions is very crucial to get substantial SV effect and current induced spin torque [3–8]. There have been several approaches for fabricating nano-scale current-driven spin valves by additive or subtractive methods [9, 10]. For additive process [9] the multi-layer is deposited onto a pre-patterned template using lift-off technique. In this method, it is difficult to control over the interface quality of the multi-layer because of the complex edge growth dynamics. On the contrary, the subtractive method in which a metal layer can be used as a mask for ion-milling process is completely free of the edge growth dynamics. It, however, needs more etching process after passivation of the junction to electrically connect the contact areas with the top electrode. An etching process essentially requires a robust etching mask [10].

The fabrication process becomes simple and efficient if we use an electron beam resist (EBR) as an etching mask in the subtractive process such as dry etching. Unfortunately, most EBRs are so vulnerable to the dry etching process that they are hard to serve as an etching mask. However, ZEP520A, a positive-tone EBR, is known to have high dry-etching resistance and its ion milling rate (0.84–0.96 Å/s) is slow enough to be used as an mask in this work.

For electron beam lithography (EBL), the proximity effect originating from the mixture of forward and backward scattering of electrons plays an essential role in determining resolution and exact shape of a pattern. The proximity effect is usually dominated by back scattering effect of the electrons from the substrates underneath the EBR [11]. Therefore, the proximity effect correction is indispensable to realize nano-sized junction patterns on a metallic multi-layer having more scattering events than semiconductors. This correction can be achieved by manipulating some exposure parameters such as dosage correction, shape correction or a combination of both [11–13]. Among them, a self-consistent technique that alters the incident dose in primitive scanning shapes into which a desired pattern is divided is used here. This technique

H. Yi · J. Chang (✉)
Center for Spintronics Research, Nano-Science Research Division, Korea Institute of Science and Technology, P.O.Box 131, Cheongryang, Seoul 130-650, Korea
e-mail: presto@kist.re.kr

requires proximity parameters, α, β, and η, which are determined experimentally using the doughnut pattern method [12, 13]. An iterative procedure should be applied to give satisfactory final results.

In this work, a set of effective proximity parameters of ZEP520A on the SV device was obtained, and a 100 nm × 100 nm sized-junction was successfully fabricated by utilizing those parameters. The effect of magnetic multi metal-layer on the proximity parameters is discussed.

Experiment

ZEP520A was spin-coated onto the magnetic metal multi-layer with spinning speed of 6,000 rpm for 60 s. The coated sample was baked at 180 °C for 2 min on a hot plate. The final thickness of the resist is about 3,000 Å. The exposure was done at accelerating voltage of 25 kV using the scanning electron microscope (JEOL FE-SEM 6500F) attached with lithography software (ELPHY PLUS, Raith GmbH). The electron beam spot size is about 10 nm. Monte-Carlo simulation (CASINO) was also performed in order to clarify the electron beam trajectory depending on the type of substrate [14].

A series of doughnut structure was patterned on both metal multi-layers on Si and bare Si substrate in order to evaluate and compare the proximity parameters of them. Each doughnut pattern consists of inner and outer circles linked with a line. The inner radius R_i and the area dose D_i are varied along x-axis and y-axis of the series of doughnut patterns respectively while the outer radius of the doughnuts R_2 is kept constant, usually in the range of four times of inner radius. Detail parameters on the doughnut structure are listed in Table 1. After exposure and development of doughnut patterns, the value of R_i for which the inner part of the doughnut is completely clearly out at each dose D_i is determined. A fitting of the curve (R_i, D_i) was carried out with the Origin 6.1 software. After obtaining the proximity parameters, we were able to perform a simulation to obtain an effective dose factor in each segment divided from the whole pattern of the device using Elphy plus software.

Table 1 Detail parameters of a set of doughnut patterns consisting of 7 × 7 array of doughnuts

No. of doughnuts in a set	49
Start radius of inner circle	0.01 μm
End radius of inner circle	3 μm
Radius of outer circle (constant)	7 μm
Start value of dose factor	0.0
End value of dose factor	20.0

The SV structure consisting of a Cu bottom electrode and a Co/Cu/Co multi-layer was deposited onto an oxidized 3,000 Å-thick SiO_2/Si substrate in an external magnetic field, using DC magnetron sputtering. The 100 nm × 100 nm sized junction in the center of the 20 μm × 20 μm squared passivation area can be defined by EBL on ZEP 520A coated metal multi-layers. In order to keep the junction size with positive tone ZEP 520A, all surroundings except the junction area should be exposed to electron beam radiation. The SV device finally can be achieved by milling out all surroundings of the junction inside the passivation area as shown in Fig. 1. The exposed pattern is inspected with both optical microscopy (Olympus AHMT-3) and SEM.

Results and discussion

Doughnut pattern and proximity parameters

Figure 2 is the SEM image of doughnut structures patterned on a ZEP520A coated metal multi-layer. It shows various doughnut shapes depending on the variation of inner radius (R_i,) and inner dose factor (D_i). Since our SEM is not equipped with the laser controlling stage, misalignment can be seen between sets of doughnut pattern. A set of doughnut pattern consisting of 7 × 7 array of doughnuts can be written on a 120 μm × 120 μm writing field without moving the stage. The line on the SEM image links all doughnuts where an inner circle completely disappears owing to the proximity effect. The R_i, and D_i of each doughnut on the line are obtained to construct the fitting curves of them using the Eq. (1) as shown in Fig. 3 [13].

$$D_{\text{center}} = D_0 = [D_i/(1+\eta)] \cdot [\exp(-(R_i/\alpha)^2) + \eta \exp(-(R_i/\beta)^2)] \quad (1)$$

where D_0 = clearing dose of the resist; D_i = dose applied during exposure; R_i = inner radius for which the doughnut is cleared out; r = lateral distance from incident electron beam; α = Standard deviation of short range scattered

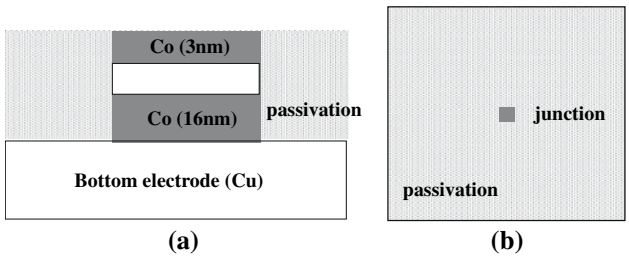

Fig. 1 A schematic view of the spin valve device after patterning. (**a**) cross-sectional view (**b**) top view

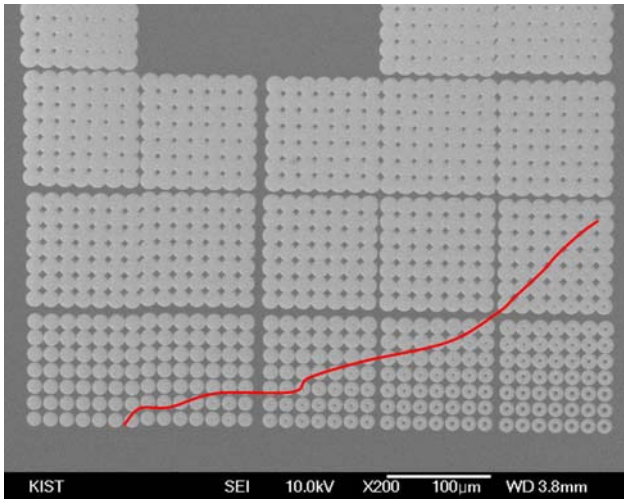

Fig. 2 SEM image of a series of doughnut structures patterned on a ZEP520A coated spin valve structure. The line on the image links the doughnut whose inner circle starts to disappear

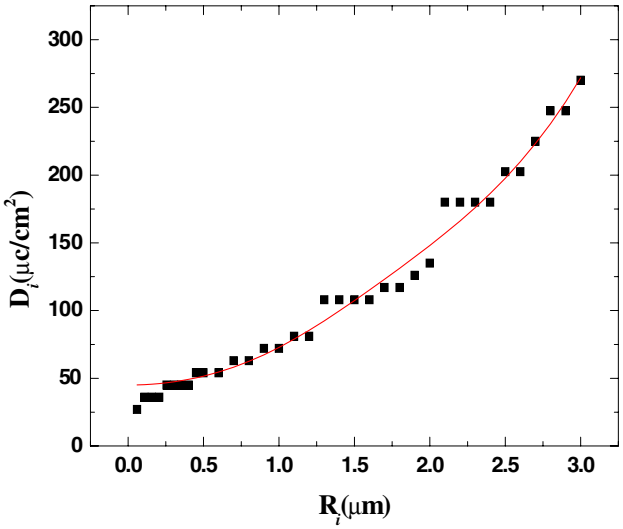

Fig. 3 The fitting curve of (R_i, D_i) got from the doughnut pattern experiment. The square points are experimental data and the solid line represents the fitting curve based on Eq. (1)

electron distribution; β = Standard deviation of long range scattered electron distribution; η = Ratio of energy deposited by short-range scattered electrons to the energy deposited by long range scattered electrons.

Two sets of proximity parameters were extracted from the SV structure on top of Si substrate and from a Si substrate without the SV structure. The resultant proximity parameters are listed in Table 2. Here the unit of α and β is μm while that of η is dimensionless. The values of ZEP 520A on pure Si substrate are quite different from those of PMMA reported previously by other groups [12, 13].

The α value of ZEP520A is much larger than that of PMMA because of the higher sensitivity of ZEP520A,

Table 2 Comparison of proximity parameters depending on the e-beam resist and substrate

	α (μm)	β (μm)	η
PMMA on SiO_2/Si	0.2–0.5	1.45–1.6	0.7
ZEP on SiO_2/Si	0.505	2.99	1.054
ZEP on the spin valve on SiO_2/Si	1.021	2.96	0.855

The proximity parameters of PMMA on SiO_2/Si substrate was previously reported by other research group [12, 13] and those of ZEP520A on spin valve multi-layers on SiO_2/Si substrate and on pure SiO_2/Si substrate was experimentally observed

which is advantageous for reducing exposure time. In general, the α value is proportional to the accelerating voltage and inversely proportional to the thickness of electron beam resist. [11] Therefore, a trade-off between resist thickness and accelerating voltage should be compromised suitably by considering both the proximity effect and the etching rate of resist. The β value of ZEP520A on Si substrate is also larger than that of PMMA. From both larger parameters of ZEP520A, it is believed that proximity effect of ZEP 520A is more critical than that of PMMA and careful control of the proximity effect is needed to realize a nano-sized pattern with exact shape and size when ZEP520A is used.

The proximity parameters of SiO_2/Si substrate without the SV structure are also compared with those of the SV. The β values ($\beta_{Si} \approx \beta_{SV} \approx 3$ μm) are almost same for the two structures while the α value of SV structure is larger than that of the Si substrate ($\alpha_{SV} \approx 1$ μm $> \alpha_{Si} \approx 0.5$ μm). According to the paper which first introduced a simple method to get a set of proximity parameters [13], the authors assumed simple substrates such as bare Si, GaAs, or light Z materials. If there were heavy Z layers on a substrate, as in our case, the model should need some modifications. One possible modification can be a triple Gaussian function, which utilizes three independent proximity parameters, α, β, and γ [15]. Here α describes the forward scattering (~30 nm) related to the resist and electron beam only, β, the short range backscattering which is introduced by the heavy Z materials (~1 μm), and γ, the long range backscattering usually from the bare substrate (~3 μm) such as Si, respectively. The triple Gaussian function is not practical to our experiment because Elphy Plus simulator we use is based on the double Gaussian function.

Another modification based on the double Gaussian function is to set the definition of the proximity parameters in a proper way. That is, α describes a short range scattering from the resist and high Z magnetic multi-layers whereas β implies the long-range scattering effect from the thick Si and SiO_2 substrate. Generally, the forward scattering within the resist is short-range one and is never

influenced by the substrate unless an extremely low voltage is used (<5 kV). Since high accelerating voltage of 25 kV and the same kind of ER were used in this work, α was little affected by forward scattering event. On the other hand, the short-range back scattering can be altered by the additional substrates introduced and it can be combined to the α value here. In order to understand the electron scattering event caused by insertion of high Z metals on Si substrate, CASINO simulation was done using on-line available program [14].

Figure 4 shows typical electron trajectories for without (a) and with the SV structure (b) on a SiO2/Si substrate simulated by the Monte Carlo simulation package CASINO. The simulation assumed electrons with 25 KeV of accelerating voltage and 10 nm of electron beam diameter.

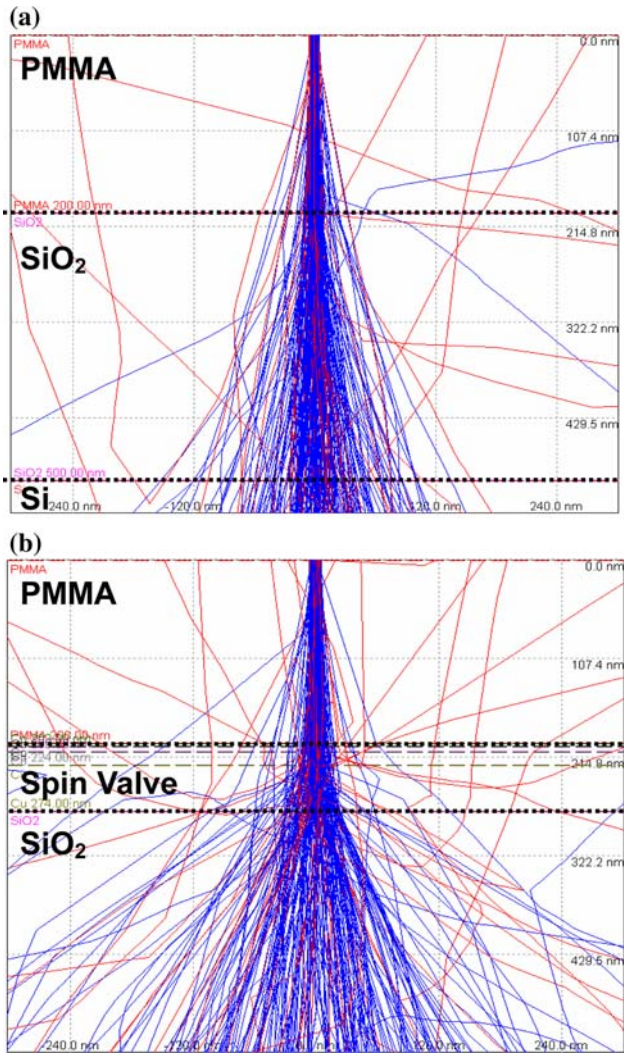

Fig. 4 CASINO simulation result at 25 KV accelerating voltage conditions. It is assumed that 200 nm thick PMMA is coated on (**a**) bare SiO_2/Si substrate and (**b**) the spin valve device on SiO_2/Si substrate

The path of incident electron beam through ER is almost same for both cases whereas the electron trajectory after penetrating the substrates becomes wider in (b) system than that of (a). That is, the electron beam path changes drastically by passing through the multi metal-layers and therefore the scattering events occur over broader ranges causing more chances of short-range backscattering event. It is believed that the short range backscattering is promoted by heavy Z materials of the multi metal-layers. Since long range backscattering is originated from the SiO2 layer, it is almost same regardless of existence of the high Z metal layer. From this simulation, we confirm that the introduction of heavy atoms of multi metal-layers influences the short-range backscattering events rather than the long range backscattering. Therefore, the change of α value in our fitting result is attributed to the increase in short-range scattering events. On the other hand, the nearly unchanged β value is thought to represent the long-range scattering from the thick bare Si substrate.

Patterning of the spin valve device with a 100 nm × 100 nm junction size

With evaluated proximity parameters of metal multi-layers summarized in Table 2, a proximity effect correction using Elphy plus system was carried out to find an effective dose factor of each segment of the pattern and the result is presented in Fig. 5. Based on the simulation, the whole pattern was divided into six segments depending on the effective dose factors. Different contrast represents a different dose factor corresponding to each segment. The thicker the contrast is, the higher the dose factor implies. The number of electrons scattered from neighbor exposing points is lower at the corner of each pattern than that of center due to the proximity effect. In order to balance the effective dose factor of each segment, the dose factor at the

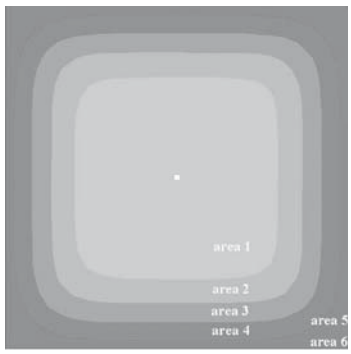

	Dose Fact or (D / D_0)
White Area	0
Area 1	1.04
Area 2	1.11
Area 3	1.22
Area 4	1.36
Area 5	1.55
Area 6	1.76

Fig. 5 Dose factor distribution of the pattern as a result of a proximity effect simulation. As the contrast becomes darker, the dose factor becomes higher

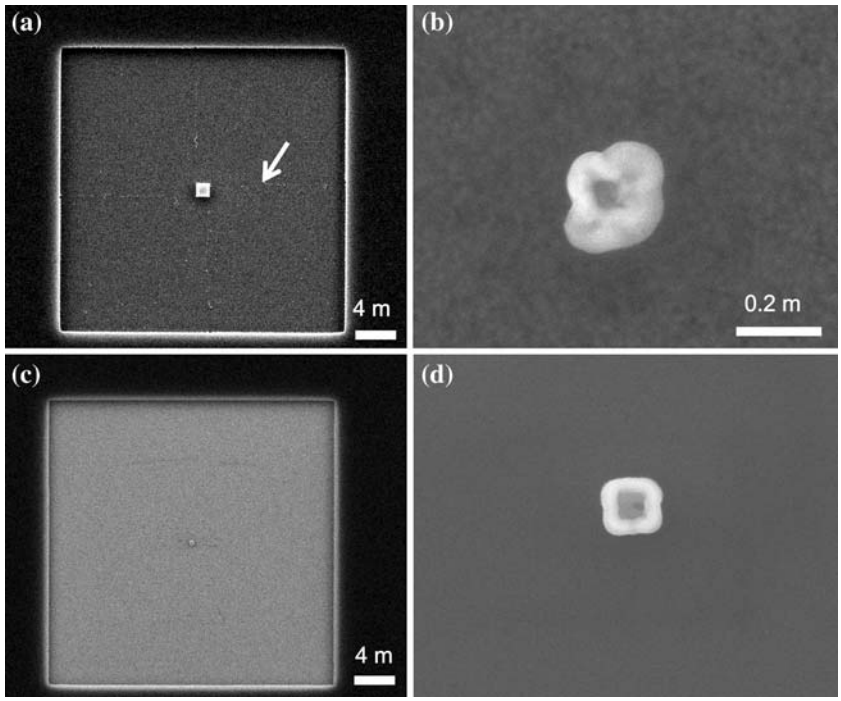

Fig. 6 Plan-view SEM images of the spin valve device fabricated without (**a**, **b**) and with (**c**, **d**) proximity correction

corner as well as at the surroundings of the pattern should be higher than that at the center.

Figure 6 presents the top view SEM image of the SV device fabricated between without and with the proximity effect correction. It shows 20 μm × 20 μm passivation area (a and c) including a 100 nm × 100 nm junction at the center (b and d). Without the proximity effect correction, there remain some residues of ZEP520A inside the passivation area (indicated by an arrow) because of an unbalanced distribution of the electron beam energy of each segment of the pattern. (Fig. 6a) Furthermore, we can also see a distorted junction shape as shown in (Fig. 6b). It is very essential to achieve a correct shape and an exact size of the junction in order to realize clear SV effect. If any residues remain in the passivation area except the junction, they act as a mask during an etching process producing some unwanted junctions in the SV device. As expected, successful proximity effect correction brings no residue in the passivation area as well as exact junction size and shape as shown in (Fig. 6c, d) Therefore, it can be concluded that the proximity effect correction is effective for fabrication of the SV device with a nano-scale junction by means of a subtractive method.

Conclusion

In the study, we successfully utilize a proximity effect correction method to realize a 100 nm × 100 nm junction size on the spin valve device. A set of the proximity parameters (α, β, and η) of ZEP520A, a positive-tone electron beam resist, is systematically investigated with a doughnut pattern method. From the fitting result, it is revealed that the short range back scattering is more critical to determine the pattern resolution than long range back scattering on the magnetic metal multi-layers and this is confirmed by the CASINO simulation. Successful modification of proximity effect based on the accurate evaluation of proximity parameters using double Gaussian function makes it possible to fabricate 100 nm × 100 nm junctions on magnetic multi metal-layers.

Acknowledgement This work was supported by ''the Korea Institutional Program in KIST.''

References

1. Grollier J, Hamzic VCA, George JM, Jaffres H, Fert A, Faini G, Youssef JB, Legall H (2000) Appl Phys Lett 78:3663
2. Albert FJ, Emley NC, Myers EB, Ralph DC, Burhrma RA (2002) Phys Rev Lett 89:226802
3. Berger L (1996) Phys Rev B 54:9353
4. Sun JZ (1999) J Magn Magn Mater 202:157
5. Katine JA, Albert FJ, Burhrman RA, Myers EB, Ralph DC (2000) Phys Rev Lett 84:3149
6. Albert FJ, Katine JA, Buhrman RA, Ralph DC (2000) Appl Phys Lett 77:3809
7. Slonczewski JC (1996) J Magn Magn Mater 159:L1
8. Tsoi M, Jansen AGM, Bass J, Chiang WC, SECK M, Tsoi V, Wyder P et al (1998) Phys Rev Lett 80:4281
9. Sun JZ, Monsma DJ, Abraham DW, Rooksmj, Koch RH (2002) Appl Phys Lett 81:2202
10. Katine JA, Albertfj, Buhrman RA (2000) Appl Phys Lett 76:354

11. Greeneich S (1980) In: Electron-beam technology in microelectronic fabrication. Academic, London, p 48
12. Wuest R, Strasser P, Jungo M, Robin F, Emi D, Jackel J (2003) Microelectron Eng 67–68:182
13. Stevens L, Jonckeere R, Froyen E, Decoutere S, Lanner D (1986) Microelectron Eng 5:141
14. http://www.gel.usherb.ca/casino/
15. Gueorguiev YM, Vutova KG, Mladenov GM (1996) Supercond Sci Technol 9:565